Design and Modeling of the Properties of the Servomechanism for a Mobile Free Space Optical Link

Jan ČIŽMÁR, Jiří NĚMEČEK

Dept. of Aerospace Electrical Systems, University of Defense, Kounicova 65, 662 10 Brno, Czech Republic

jan.cizmar@ unob.cz, jiri.nemecek@unob.cz

Abstract. *The paper deals with the design of a tracking system determined for mobile free space optical link communication system. The paper also contains description of two-step method of the optical-axes pointing process, description of the basic properties of servomechanisms and results of the simple simulation of the tracking-system function model. The entire model consists of four partial models, i.e. of model of trajectory, model of uneven road surface, model of vehicle and model of horizontal and vertical servos. Results of these simulations will be used to give precision to the construction design of the mobile free space optical link station and its servomechanisms.*

Keywords

Free space optical link, communication, pointing, tracking, servomechanism, inertial reference unit, TV camera, modeling, simulation.

1. Introduction

Currently, Free Space Optical (FSO) links are a widespread method of telecommunication. They are mostly used to connect two stationary stations kilometers apart, where the transmission signal is often carried by laser radiation. In practice, the implementation requirements for a FSO link between two stations are becoming more demanding, focusing on at least one of the stations being placed on a moving vehicle (car, plane, boat, etc.).

When using FSO links, it is necessary to align the optical axes of the optical signals for both station receivers and transmitters with sufficient accuracy.

The required accuracy of the optical axes is primarily determined by the spatial characteristics of the laser beams and the field of view of the receivers, but also by the current state of the atmospheric space between the communicating stations. This issue was discussed in detail in literature [1]-[7].

2. Tracking System of MFSO

In cases where either or both land mobile FSO (MFSO) stations are located on a moving vehicle, it is necessary to set the accuracy of the optical axes for both communicating stations (1 and 2). Additionally, it is also necessary to set the initial (approximate) directional orientation of the optical axes, for both activation of the communication system, and also in case the MFSO communicating stations lose their mutual visibility.

Therefore, both MFSO stations must be equipped with two servomechanisms to ensure their movement around two mutually perpendicular axes $Y_{1/2}$ and $Z_{1/2}$ of the Body Coordinate Systems (BCS), see Fig. 1. The origins of both BCS systems $0_{1/2}X_{1/2}Y_{1/2}Z_{1/2}$ are identical with the Earth Coordinate Systems (ECS) $0_{G1/2}X_{G1/2}Y_{G1/2}Z_{G1/2}$. The axes $X_{G1/2}$ points to the North, $Y_{G1/2}$ points to the East, and all of them are perpendicular to the local vertical axes. The axes $Z_{G1/2}$ lies on the local vertical axes and points to the Earth's center.

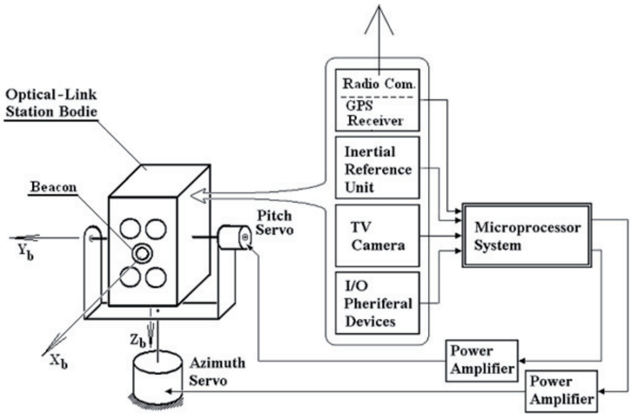

Fig. 1. Structure of a moving FSO station.

Control of the angular motion of the optical axes is therefore proposed as a two-stage process. It is calculated for the distance in kilometers, the most commonly used FSO distance, where the Earth can be considered a sphere with radius of $R_E \cong 6367445$ m. The radius is determined as an arithmetic average of both the large and the small half-axes of the referenced Earth ellipsoid WGS84. [8]

The first auxiliary control stage is the so called "coarse pointing" of the stations and is carried out by GPS measurement of the position of both MFSO stations [9].

Then, both MFSO stations exchange information about their location via radio transmission (latitude $\varphi_{1/2}$ and longitude $\lambda_{1/2}$ and ellipsoidal height $h_{1/2}$):

$$L_{1/2} = \left(\varphi_{1/2}, \lambda_{1/2}, h_{1/2}\right). \quad (1)$$

Based on this information, the North $n_{1\text{-}2/2\text{-}1}$, East $e_{1\text{-}2/2\text{-}1}$ and the vertical $h_{1\text{-}2/2\text{-}1}$ distance components are set in the MFSO microprocessor station circuits and the final distance s between the stations can be calculated.

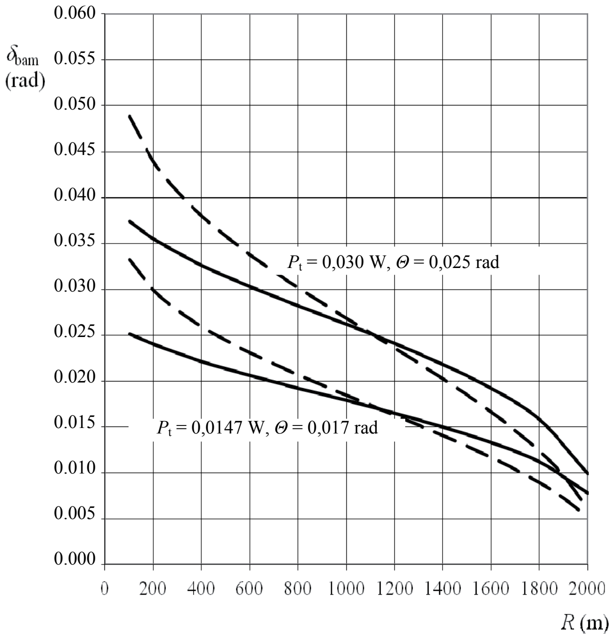

Fig. 2. Angular deviation limits of the Gaussian (---) and the Top Hat beam (-) - considering atmospheric interference.

For these calculations, the following formulas are true:

$$n_{1-2/2-1} = R_{\mathrm{E}}\left(\varphi_{2/1} - \varphi_{1/2}\right), \quad (2)$$

$$e_{1-2/2-1} = R_{\mathrm{E}} \cos\left(\frac{\varphi_{2/1} - \varphi_{1/2}}{2}\right)\left(\lambda_{2/1} - \lambda_{1/2}\right), \quad (3)$$

$$h_{1-2/2-1} = h_{2/1} - h_{1/2}, \quad (4)$$

$$s_{2-1/1-2} = s = \sqrt{n^2_{1-2/2-1} + e^2_{1-2/2-1} + h^2_{1-2/2-1}}. \quad (5)$$

Then, the mutual directional alignment of both stations $\psi_{\mathrm{r}1\text{-}2/2\text{-}1}$, i.e. the required rotations around the ECS axes $0X_{\mathrm{G}1/2}Y_{\mathrm{G}1/2}Z_{\mathrm{G}1/2}$ of the two stations, is given by the following formulas:

$$\psi_{\mathrm{r}1-2/2-1} = \frac{\pi}{2} - \operatorname{arctg}\frac{n_{1-2/2-1}}{e_{1-2/2-1}}, \quad e_{1-2/2-1} \geq 0, \quad (6)$$

$$\psi_{\mathrm{r}1-2/2-1} = \frac{3\pi}{2} - \operatorname{arctg}\frac{n_{1-2/2-1}}{e_{1-2/2-1}}, \quad e_{1-2/2-1} < 0. \quad (7)$$

Then, the following formula is true for the required rotation angles $\vartheta_{\mathrm{r}1\text{-}2/2\text{-}1}$ around the axes $Y_{\mathrm{G}1/2}$:

$$\vartheta_{\mathrm{r}1-2/2-1} = \frac{h_{2/1} - h_{1/2}}{s}. \quad (8)$$

The angles $\psi_{\mathrm{r}1\text{-}2/2\text{-}1}$ and $\vartheta_{\mathrm{r}1\text{-}2/2\text{-}1}$ are calculated in the local ECS $0_{\mathrm{G}1/2}X_{\mathrm{G}1/2}Y_{\mathrm{G}1/2}Z_{\mathrm{G}1/2}$, where the axis $X_{\mathrm{G}1/2}$ is pointing to the North, axis $Y_{\mathrm{G}1/2}$ is pointing to the East, and both of them are perpendicular to the local vertical axis. The axis $Z_{\mathrm{G}1/2}$ is the local vertical axis and points towards the Earth's center.

The current position of both communicating MFSO station bodies is measured using miniature inertial reference units (IRU) with micro-electro-mechanical sensors (MEMS). The IRU provides all information about the body position angles of the MFSO station that are affecting the system along the axes of the station's BCS, i.e. the roll $\phi_{\mathrm{a}1/2}$, the pitch $\vartheta_{\mathrm{a}1/2}$, the magnetic heading $\psi_{\mathrm{a}1/2}$, the vectors of angular velocity and the linear acceleration [8], [10].

The differential angles between the required and the actual position of the optical axis are represented by the angle change signals $\delta_{\mathrm{GH}1/2} = \psi_{\mathrm{r}1/2} - \psi_{\mathrm{a}1/2}$ and $\delta_{\mathrm{GV}1/2} = \vartheta_{\mathrm{r}1/2} - \vartheta_{\mathrm{a}1/2}$, by which the MFSO bodies, respectively, must be rotated using a servo.

All of these above mentioned angles are provided in the ECS, whereas the servo axes are identical with the body coordinate system. Therefore, when the vehicle carrying the MFSO station moves or the stationary MFSO station is inaccurately placed, it is necessary to transform the signals $\delta_{\mathrm{GV}1/2}$ and $\delta_{\mathrm{GH}1/2}$ from the ECS into the BCS using the following formulas:

$$\delta_{\mathrm{V}1/2} = \delta_{\mathrm{GV}1/2}\cos\phi_{1/2} + \delta_{\mathrm{GH}1/2}\sin\phi_{1/2}\cos\vartheta_{1/2}, \quad (9)$$

$$\delta_{\mathrm{H}1/2} = -\delta_{\mathrm{GV}1/2}\sin\phi_{1/2} + \delta_{\mathrm{GH}1/2}\cos\phi_{1/2}\cos\vartheta_{1/2}.. \quad (10)$$

The second control stage called "fine pointing" of both stations is carried out through measuring light beacon image deviations from the optical axis of the CCD (Charge Coupled Device) camera. Using a suitable image processing method, the magnitudes of the angular deviations, i.e. the rotation angles around the axes $Z_{1/2}$ and $Y_{1/2}$ of the BCS of both MFSO stations, are then assessed in the microprocessor systems of the MFSO stations.

3. Proposed Structure of the Tracking Servos

In order to maintain availability of the MFSO link, it is necessary to ensure sufficient accuracy and speed of the servomechanisms. The MFSO must be able to mutually align their optical axes while the vehicle is moving. The required targeting accuracy analyzed in [4] shows that for FSOs built for the distance of 2000 m, it is necessary to ensure alignment accuracy of the laser beam axes to be better than 5 mrad (17.2 '), see Fig. 2.

To meet such difficult requirements, servos of the PID controller (Proportional-Integral-Derivative) type were designed. The block diagram of the proposed horizontal and vertical servos is shown in Fig. 3.

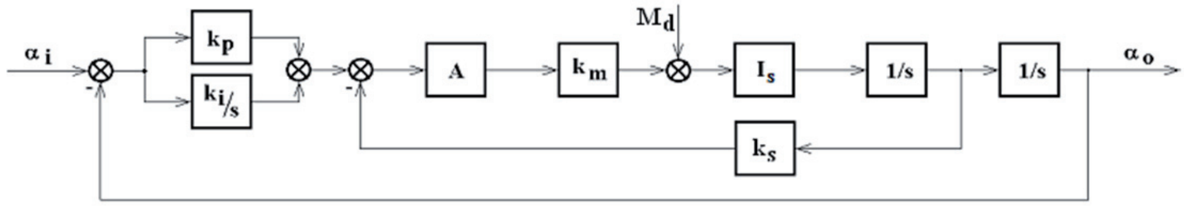

Fig. 3. Block diagram of the MFSO station servomechanisms.

The abbreviations indicate: A is the overall gain of the amplifier (100), k_m is the actuator gain (30 Nm / V), I_s is the moment of inertia of the MFSO station with servos (0.15 kg m^2 and 0.2 kg m^2 are calculated from catalogue data for a particular weight and dimensions of the three different FSO stationary stations), k_s is speed feedback gain (0.4 V / rad / s), k_p is proportional feedback gain (30 V / rad), k_i is integral feedback gain (10 V s / rad), α_o is output angle, α_i is signal for the required angle of servo rotation, M_d is disturbance torque.

The Laplace image of the transfer function describing transmission under the required angle is as follows:

$$F_\alpha(s) = \frac{\alpha_o(s)}{\alpha_i(s)} = \frac{\frac{k_p}{k_i}s+1}{\frac{1}{Ak_m I_s k_i}s^3 + \frac{k_s}{k_i}s^2 + \frac{k_p}{k_i}s + 1} \quad (11)$$

where s is the Laplace´s operator.

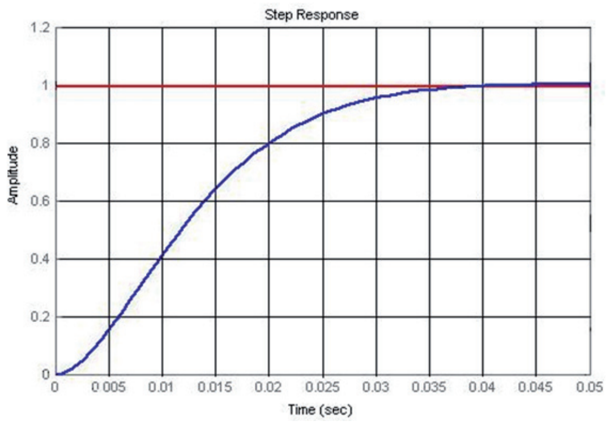

Fig. 4. Servo's response to the unit step input.

It is clear from the transfer function that the servo gain is equal to 1. Dynamic properties are characterized as a response to a step change, graphically depicted in Fig. 4.

The Laplace image of the transfer function describing the transmission of the disturbance torque M_d is as follows:

$$F_\alpha(s) = \frac{\alpha_o(s)}{M_d(s)} = \frac{\frac{1}{Ak_i k_m}s}{\frac{1}{Ak_m I_s k_i}s^3 + \frac{k_s}{k_i}s^2 + \frac{k_p}{k_i}s + 1}\,. \quad (12)$$

This formula implies that the steady-state deviation is zero.

4. Model of the MFSO Link Tracking System

A computer model for verifying dynamic properties of both MFSO servomechanisms was developed in the Matlab – Simulink environment. This model consists of the following functional blocks, see Fig. 5:

1) A block for input data,
2) A block for a vehicle trajectory model,
3) Blocks for horizontal and vertical servo models,
4) Blocks for horizontal and vertical vehicle movement models,
5) A block for output data display and evaluation.

The block for input data is used for easy input of the optional model parameters such as: the actual disturbance torque of the horizontal and vertical servos M_h and M_v, vehicle speed V, minimum passing distance of the stations R_{min}, average size road surface unevenness I_r, average distance between road surface unevenness M_r, and the height difference between the stations ΔH.

The movement of one of the MFSO stations along a straight horizontal trajectory was modeled and used as a servo actuating signal. In one particular case, the mobile MFSO station (or a vehicle carrying it) passed the stationary station at a minimum distance of R_{min} = 100 m, with a speed of 50 km/h, where the stationary station was located ΔH = 5 m higher than the mobile station, due to the trajectory of the mobile station. The start and the end points of the simulation were on the trajectory of the moving station, and the distance between the mobile and fixed MFSO station was 2002.5 m. The corresponding servo control signals of the fixed MFSO station were generated in the vehicle trajectory model block.

The model blocks for the vertical and horizontal servomechanisms are basically identical. The models represent servomechanisms with derivative, proportional and integral feedback, the structure of which was described above.

In the model block for the horizontal and vertical vehicle disturbance torque, a random disturbance signals

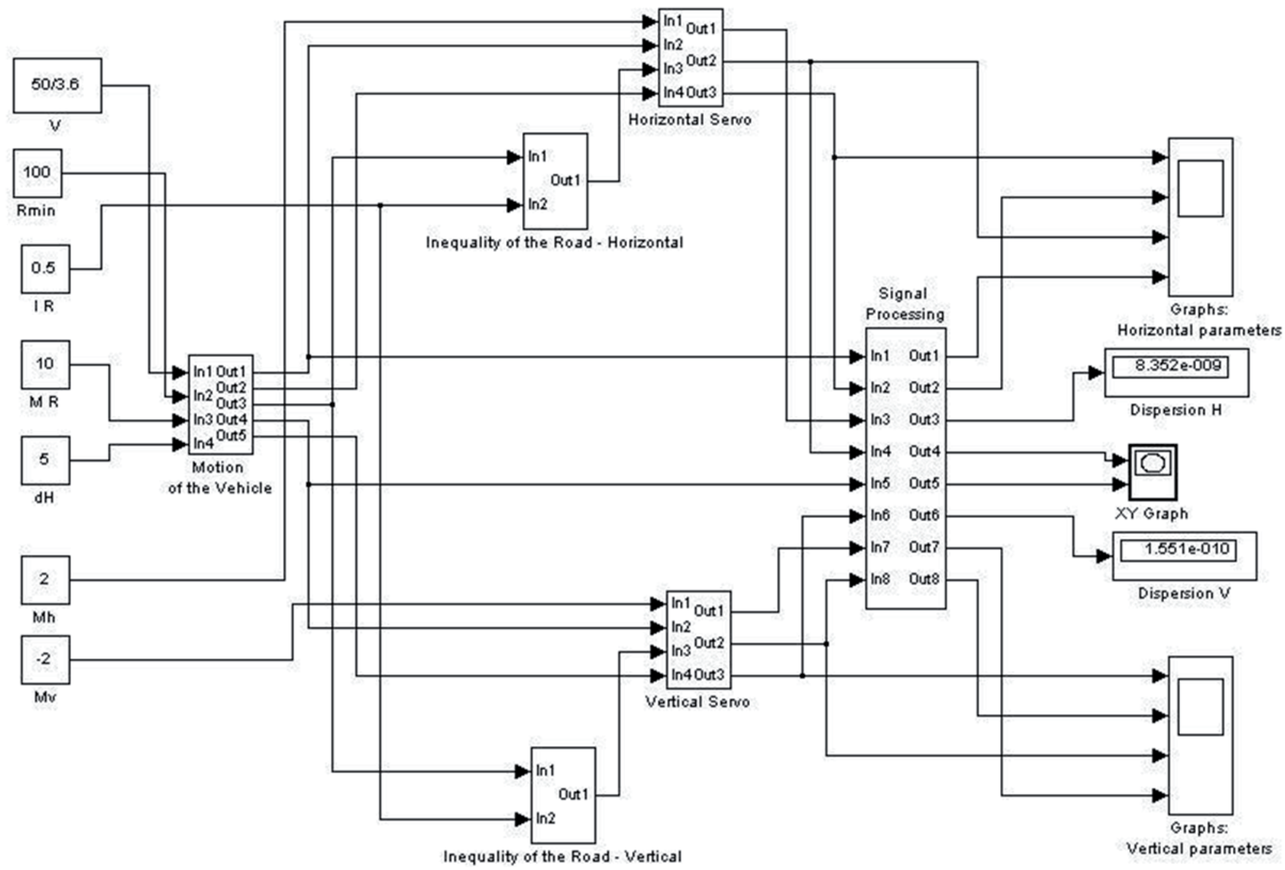

Fig. 5. Diagram of the MFSO model in the Matlab – Simulink environment.

were generated representing the unevenness of the road, see the following formula:

$$h_r(s) = F_r(s) h_{WN}(s) = \frac{I_r c_a \left(\frac{M_r}{V} \right)^{-c_b}}{\frac{M_r}{V} s + 1} h_{WN}(s) \quad . \quad (13)$$

Uneven road surfaces are defined by an average bump height and by an average bump distance. Their value at a particular moment is simulated by white noise filtration (dyeing).

For that calculation, a transfer function of the inertial element of the first order was used, where the gain I_r was equal to medium-size road bumps and the time constant T was given by an average distance between the bumps M_r divided by the vehicle speed V; i. e. $T = M_r / V$. Symbols c_a and c_b represent realistic numbers defined by the ratio of model calculation steps Δt and the time constant $T = M_r / V$, that is $\Delta t / T$. The actuation signal is white noise h_{WN}. Then, the signal h_r creates angular oscillations of the vehicle $\beta_v(t)$ that is simply represented by an oscillating member of the second order as follows:

$$\beta_v(s) = F_v(s) h_r(s), \quad \frac{1/(2G)}{T_v^2 s^2 + 2\xi_v T_v s + 1} h_r(s) \quad (14)$$

where β_v is angular deviation, $G = 1.75$ m is the vehicle wheel-track, $T_v = 0.1$ s is the car oscillation time constant and $\xi_v = 0.4$ is dumping coefficient of these oscillations. Then, the angular vehicle movements are transferred through the friction moments in the Cardan suspension bearings of the MFSO station.

These moments were modeled by a block simulating dry and viscous friction called Coulomb & Viscous Friction which is a part of the SIMULINK environment toolbox. The dry friction was set to the value of 1 Nm and the viscous friction to 0.2 N m rad^{-1} s. In the axes of both servos, there are constant disturbance torques of 0.2 N m.

In the signal processing block, the output signals are represented through the standard deviations of the MFSO optical axis pointing errors in both horizontal and vertical directions. The angles and angle speeds of the MFSO-station deviation and the performance of both servos are graphically depicted in Fig. 6.

5. Conclusion

The initial condition and assumption for creating this model was a perfect static and dynamic balance of the two servo systems as well as of the MFSO station body and the axes Y_B, Z_B. The model takes into account only the following errors: errors caused by the vehicle's "primary motion"

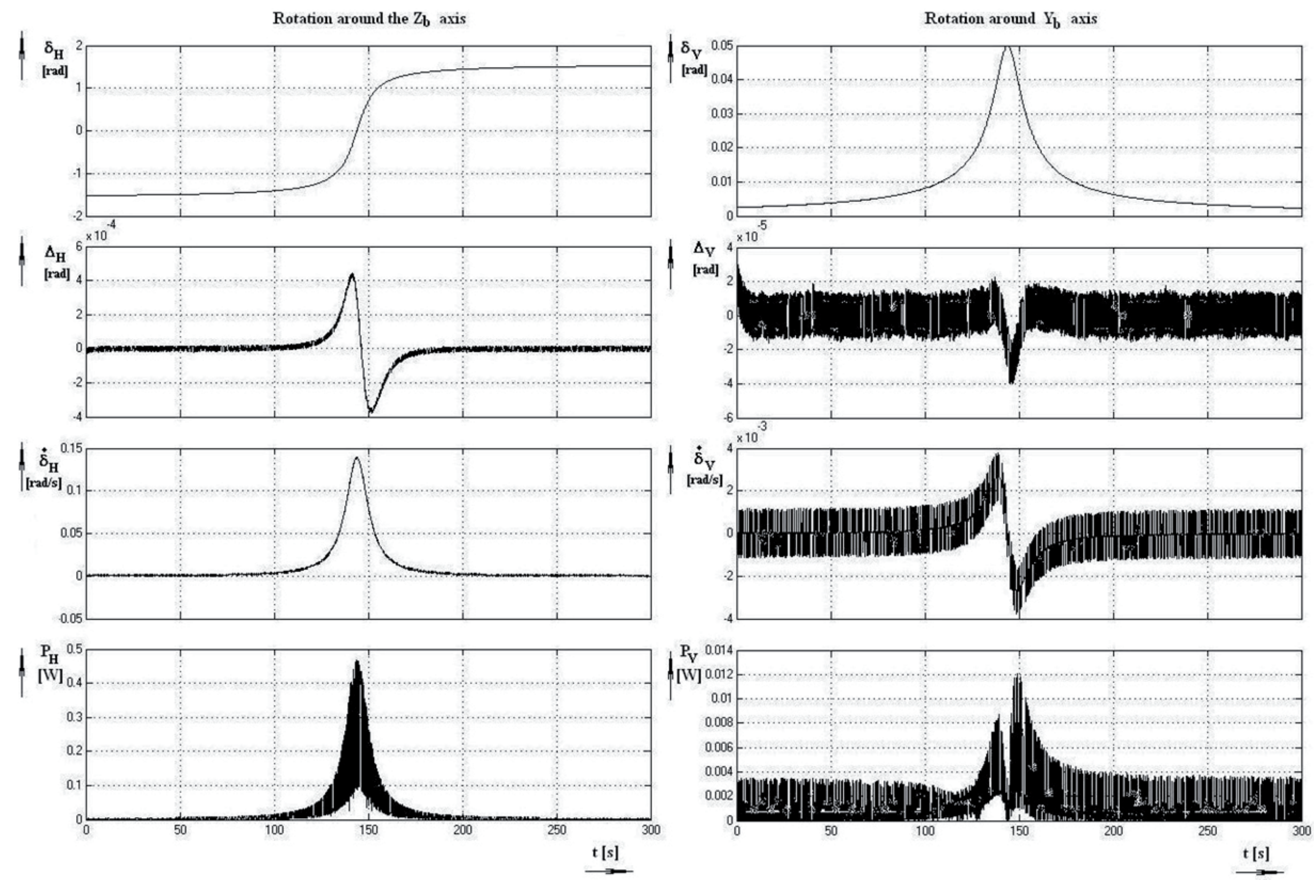

Fig. 6. Diagram of the MFSO model in the Matlab – Simulink environment.

on a straight trajectory; errors caused by the vehicle's "secondary motion" on an uneven road that is transferred though the friction moments in the bearings of Cardan suspension; and a static torque effect along the axes of the Cardan suspension.

The results of the modeling are clear from the diagrams in Fig. 6, showing the horizontal and vertical servo deviations δ_H, δ_V; the angle positioning errors Δ_H, Δ_V; the angle deviation speeds $\dot{\delta}_H, \dot{\delta}_V$ and powers P_H, P_V.

The maximum optical-beam pointing errors of $\Delta_H \approx 4 \cdot 10^{-4}$ rad and $\Delta_V \approx -4 \cdot 10^{-5}$ rad were taken at times of the MFSO maximum angle acceleration, with the following experiment conditions of ($I_r = 0.5$ m, $M_r = 10$ m, $R_{max} = 2002.5$ m, $R_{min} = 100$ m, $\Delta H = 5$ m, $V = 50$ km/h, $M_H = 2$ Nm, and $M_H = -2$ Nm). These calculated angle errors of the servo setting are substantially smaller than the maximum possible errors for which the FSO is still available (see above Section 3 about FSO availability). The reason for these errors is mainly inertia of both the servo system and the MFSO station body.

Under experimental conditions, the disturbance caused by the vehicle motion on an uneven road had only a minimum effect on the precision of optical-beam pointing. Similarly, the constant torques in the servo axes have only a minimum effect on the system.

In the near future, the research team will conduct practical measurements and recordings of signals caused by vehicle motion, using Integra inertial reference unit produced by the TL-Elektronic Company. All the measurements will be subsequently evaluated. The present model will also be supplemented with a model representing disturbance elements caused by both the MFSO-station body system imbalance and the servomechanisms imbalance.

Acknowledgements

The paper was written under the auspices of the Project Development Department of the University of Defense – Project K206 named "Complex Electronic System for UAS", and supported by the association UDeMAG (University of Defense MATLAB Group).

References

[1] WILFERT, O. *Wireless Optical Links*. Brno: Brno University of Technology, 2004, 93 p. (In Czech)

[2] HENNIGER, H., WILFERT, O. An introduction to free-space optical communication. *Radioengineering,* 2010, vol. 19, no. 2, p. 203 – 212.

[3] NĚMEČEK, J., ČIŽMÁR, J. Control system for positioning of a transmitter optical beam and a receiver field of view for a mobile free space optical link. In *Proceedings of 5th International Symposium Advances in Mechatronics (AiM 2010)*. Trencin (Slovakia), 2010, p. 55 – 59.

[4] ČIŽMÁR, J., NĚMEČEK, J. Requirements for control system of mobile free space optical link. *Advances in Military Technology*, 2012, vol. 7, no. 1, p. 69 – 79.

[5] MAO, XIA, LIU, YAN. Optical axis stabilization of a two-axis platform. In *WRI Global Congress on Intelligent Systems GCIS '09*. Xiamen (People´s Republic of China), 2009, vol. 2, p. 274 to 278.

[6] FARID, A. A., HRANILOVIC, S. Outage capacity optimization for free-space optical links with pointing errors. *Journal of Lightwave Technology*. 2007, vol. 25, no. 7, p. 1702 – 1710. [Online] Cited 2009-03-26. Available at: http://www.ece.mcmaster.ca/~hranilovic/publications/articles/07/jlt06IEEEFinal.pdf.

[7] POLIAK, J., PEZZEI, P., LEITGEB, E., WILFERT, O. Analytical expression of FSO link misalignments considering Gaussian beam. In *Proceedings of the 2013 18th European Conference on Network and Optical Communications & 2013 8th Conference on Optical Cabling and Infrastructure (NOC-OC&I)*. Graz (Austria), 2013, p. 99-103.

[8] TITTERTON, D. H., WESTON, J. L. *Strapdown Inertial Navigation Technology.* 2nd ed. Lexington (USA): MIT Lincoln Laboratory, 2004.

[9] JAKUBOV, O., KOVÁŘ, P., KAČMAŘÍK, P., VEJRAŽKA, F. The witch navigator - A low cost GNSS software receiver for advanced processing techniques. *Radioengineering*, 2010, vol. 19, no. 4, p. 536 – 543.

[10] JALOVECKÝ, R., ČIŽMÁR, J. ŠKVAREK, An Inertial Reference Unit – development and testing. In *2nd International Scientific Conference on Special Technology 2008.* Bratislava, (Slovakia), April 2008, vol. 2, p. 48-52.

About Authors ...

Jan ČIŽMÁR was born in Brno in 1953. He graduated from Antonin Zapotocky Military Academy in 1976. In 1981 he passed through a selection procedure for a lecturer position at Antonin Zapotocky Military Academy. He has worked at the University of Defense up to this day. In 1991 he received the Ph.D. degree in Measuring Technology. In 2008 he habilitated as an associate professor with the thesis "Modeling of Inertial Navigation Systems". His pedagogic, scientific and publication activities are focused into the spheres of measurement of physical values, flight instruments, avionics, oxygen equipment, and air conditioning systems of the aircraft.

Jiří NĚMEČEK was born in Vyškov in 1959. In 1984 he graduated from the Military Air University in Košice. In the same year he started to work as a lecturer at the Dept. of Special Equipment at the mentioned college. From 1990 to 2009 he worked as a lecturer at the Military Academy and the University of Defense in Brno. Nowadays he is a lecturer of Special Systems and Armament at the Dept. of Aerospace Electrical Systems. In 1993 he received the Ph.D. degree in Measuring Technology. His pedagogical work is focused on the area of air sighting systems and air missiles. His scientific and research activities are aimed at problems of the free space optical links dependability and protection of the aircraft against the missiles.